Ionization of Atoms by the Spatial Gradient of the Pondermotive Potential in a Focused Laser Beam

E. Wells,[1] I. Ben-Itzhak,[2] and R. R. Jones[1,*]

[1]*Department of Physics, University of Virginia, Charlottesville, Virginia 22904-4714, USA*

[2]*J.R. Macdonald Laboratory, Department of Physics, Kansas State University, Manhattan, Kansas 66506, USA*

(Received 9 November 2002; published 6 July 2004)

Ionization of atoms by the spatial gradient of the pondermotive potential in a focused laser beam is investigated. Rydberg ions, formed during the interaction of noble gas atoms with an intense laser pulse, are used to probe the gradient field. Rydberg ion species with higher ionization potentials are produced at locations where the gradient field is largest. The measured Rydberg ion yields differ dramatically from estimates that ignore gradient-field ionization, but are in good agreement with predictions that include the effect.

DOI: 10.1103/PhysRevLett.93.023001 PACS numbers: 32.80.Rm, 32.80.Wr

The response of atoms, molecules, and clusters to intense laser light continues to be a topic of considerable interest [1–4]. Experiments designed to study strong field phenomena rely on tight focusing to achieve high laser intensities. Almost invariably, the spatial dimensions of the laser focus are smaller than the gaseous target. Consequently, in any given laser shot, target particles experience peak intensities ranging from zero (outside the focus) to some maximum (at the center of the focus). The unavoidable integration of experimental signal over the laser focal volume is a well recognized problem, and a number of techniques have been implemented to reduce its effects [5]. However, the variation in laser intensity over the volume of a single target particle is typically neglected and, therefore, any physics associated with the laser intensity gradient is implicitly ignored.

It is well known that a spatially varying laser intensity can have a significant effect on the mechanical motion of neutral particles and electrons. Atoms, molecules, and larger objects can be trapped, guided, and otherwise manipulated by light forces associated with the gradient of an intensity-dependent potential energy function [6]. The electric field in a laser beam induces an oscillating dipole moment within each neutral particle, and the time-averaged potential energy of the dipole in the laser field is proportional to the cycle-averaged laser intensity. Any spatial intensity variation in the light beam results in a proportional force on the neutral particle due to the gradient of the dipole potential. Similarly, free electrons acquire a "wiggle" energy associated with their periodic motion in an oscillating laser field. The time-averaged wiggle energy is the pondermotive potential, $U_p = 2\pi\alpha I/\omega^2$, where I is the cycle-averaged laser intensity, ω is the laser frequency, α is the fine-structure constant, and all equations are in atomic units unless otherwise noted. Any spatial variation in I results in a pondermotive force, $\vec{F}_\nabla = -\nabla U_p$, that, as first recognized by Kapitza and Dirac [7], can scatter free electrons [8,9]. A classical field, $\vec{F}_\nabla = \nabla U_p$, can be defined as the source of the pondermotive force on an electron.

In spite of the fact that it is commonly neglected, this pondermotive-gradient field can have a substantial magnitude under currently accessible experimental conditions, and therefore might affect the dynamic evolution of *bound* as well as free electrons in typical experiments (see Fig. 1). Consider an 800 nm Ti:sapphire laser pulse focused to a 1 μm diameter waist (FWHM) with a peak intensity $I = 10^{19}$ W/cm^2. In this case, the gradient field has a maximum magnitude $F_\nabla \sim 1$ a.u. or $\sim$6% of the peak oscillating field in the laser pulse. Under the same focal conditions, at $I = 10^{15}$ W/cm^2, $F_\nabla \sim 10^{-4}$ a.u. This field is 3 orders of magnitude smaller than the peak laser field. It may, however, still have an impact on electron dynamics within a target atom or molecule due to the important role played by transient excited-state

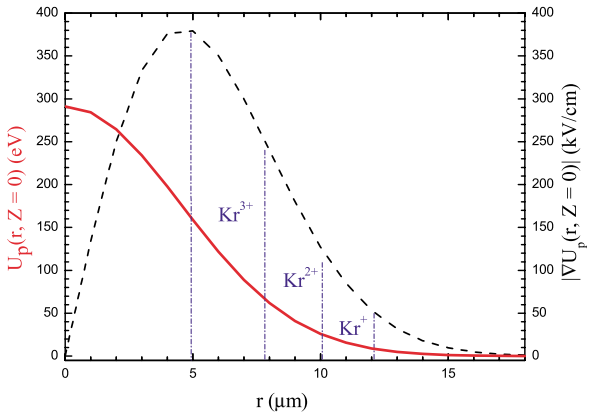

FIG. 1 (color online). U_p (solid curve) and ∇U_p (dashed curve) in the focal plane of a Gaussian beam, plotted as a function of distance, r, from the beam axis for typical experimental conditions at a peak intensity of 5×10^{15} W/cm^2. Spatial regions where different charge states of Kr are produced are noted. Above their saturation intensities, ions are produced in the wings of the focal volume where higher IP species experience greater gradient fields.

 0031-9007/04/93(2)/023001(4)$22.50

resonances in many strong-field processes [10]. For example, an electron with principal quantum number $n > 5$ will leave the atom via "over the barrier" field ionization in a gradient field of only 10^{-4} a.u.

We consider the influence of F_∇ on Rydberg ions that are produced during the exposure of noble gas atoms to focused laser pulses with peak intensities of 10^{16} W/cm^2. During the intense laser pulse, the pondermotive potential transiently shifts excited states through multiphoton resonance with the ground state [10]. Population transferred to low-lying states rapidly ionizes, resulting in resonance-enhanced structure in above-threshold ionization (ATI) electron spectra. However, since efficient photoabsorption requires that the electron have a high probability of passing within a few a.u. of the nucleus, the population transferred to high-lying Rydberg states does not readily photoionize. Moreover, during one-half of an optical-field cycle, a slow moving Rydberg electron has insufficient time to travel over or through the laser-modified binding potential barrier and, therefore, tunneling ionization does not occur. Instead, quite remarkably, probability amplitude trapped in high-lying Rydberg states can be immune to ionization even at laser intensities great enough to strip multiple electrons from the atom [11]. In fact, the generation of a pulsed x-ray gain medium, based on laser stripped Rydberg ions, has been proposed [12]. However, as discussed in more detail below, Rydberg ions are very sensitive to quasistatic electric fields and will ionize in a relatively weak pondermotive-gradient field.

In the experiment, 35 fs, 780 nm laser pulses are directed into a high vacuum chamber (base pressure 5×10^{-10} torr) and focused using a 5 cm spherical mirror. The chamber is backfilled with Ar, Kr, or Xe at pressures of 10^{-9} to 10^{-6} torr. The target atoms interact with the focused laser beam between two parallel field plates. A weak static field $F_e = 70$ V/cm pushes ions formed by the laser into a second field region. Here, Rydberg ions are further ionized by a stronger field, $F_i = 7.6$ kV/cm. The ions then travel through a field-free drift region before striking a microchannel plate detector. Because the Rydberg ions change their charge state in the second field region, they are easily distinguished from other ions by their time-of-flight (TOF) in the spectrometer. Data are collected using a multichannel scalar (MCS) as described in Ref. [13] and a typical TOF spectrum is shown in Fig. 2. To eliminate space charge effects and detector saturation, the target gas pressure is adjusted so that fewer than one count per ion peak is detected for any given laser shot. Negligibly small numbers of Rydberg ions are produced using circularly polarized light [11]. Thus, TOF spectra acquired with circular polarization are used to unambiguously identify Rydberg ion peaks in the linear polarization data. Moreover, the ion yields obtained with circular polarization are free of nonsequential ionization effects and, therefore, can be compared to Ammosov-Delone-Krainov (ADK) tunneling theory to calibrate the

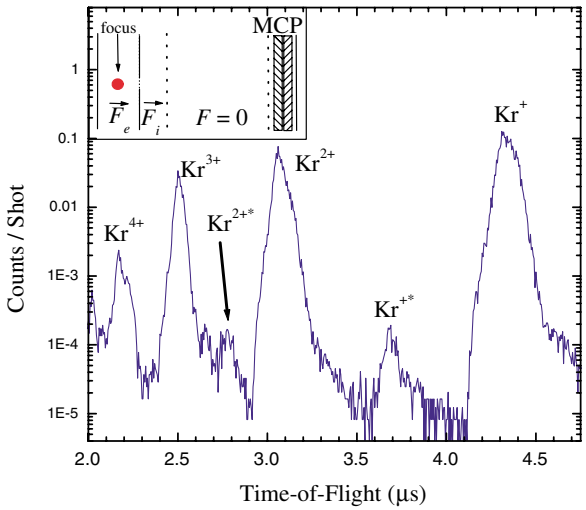

FIG. 2 (color online). A typical time-of-flight spectrum for Kr. The inset shows a schematic of the TOF spectrometer.

peak focused laser intensity [14]. Accurate numerical modeling of the laser intensity variation throughout the focal volume is enabled by imaging the laser focus with a charge-coupled device camera. Using the measured beam characteristics, the ADK intensity calibration indicates that the laser pulse duration is closer to 70 fs throughout the astigmatic laser focus and, therefore, this value is used in the numerical simulations described below.

With linear laser polarization, singly and doubly charged Rydberg ions are observed for Xe, Kr, and Ar targets. Each Rydberg ion species, $A^{(Z-1)+*}$, has an effective appearance intensity set by memory limitations in the MCS. Below the appearance intensity, a statistically insignificant number of $A^{(Z-1)+*}$ Rydberg ions are counted before the buffers associated with lower charge states are filled. The appearance intensities are comparable to, or greater than, the saturation intensities for the bare ions A^{Z+}. Above the appearance intensity for each species, greater numbers of Rydberg and bare ions are produced and, as shown in Fig. 3, the ratio of detected Rydberg ions $A^{(Z-1)+*}$ to bare ions, A^{Z+}, is roughly independent of intensity for all target atoms [11]. This observation indicates, not unexpectedly, that the processes responsible for the production of $A^{(Z-1)+*}$ and A^{Z+} ions have the same order of nonlinearity, and that these species originate from the same regions within the laser focal volume. We refer to each ratio, $A^{(Z-1)+*}$:A^{Z+}, as the normalized Rydberg yield for that species. Because the tunneling ionization rates for noble gas atoms and ions are well known [14], the charge of a Rydberg ion provides a convenient measure of the peak intensity and the gradient field to which it has been exposed.

The data in Fig. 3 show that species with higher ionization potentials (IPs) have smaller normalized Rydberg yields (Xe^{2+*}:Xe^{3+} is an exception). Accordingly, no Rydberg ions $A^{(Z-1)+*}$ with $Z > 3$ are observed. Moreover, because the data in Fig. 3 are acquired above the saturation intensity for the associated bare-ion

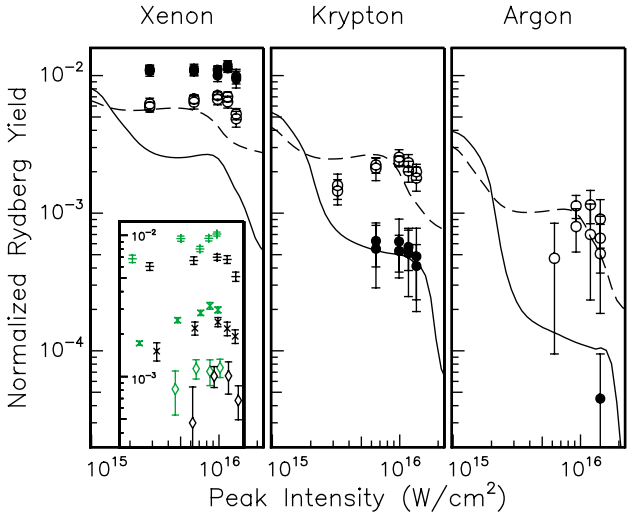

FIG. 3 (color online). Normalized Rydberg yields vs laser intensity for Xe, Kr, and Ar. Open (filled) circles and dashed (solid) lines correspond to the experimental and simulated A^{+*}:A^{2+} (A^{2+*}:A^{3+}) ratios, respectively. The simulated yields at the extreme left of each plot correspond to the intensity-independent results ignoring gradient-field ionization. The calculated low-intensity yields are not identical for each species due to the different Rydberg ion detection efficiencies and the energy normalization factors from Eq. (1). The simulated yields decrease sharply at two different intensities, corresponding to the onset of gradient-field ionization in two distinct spatial regions near the sagittal and tangential foci of the astigmatic beam. Inset: A^{+*}:A^{2+} ratios measured with two different focusing geometries for Xe (+), Kr (×), and Ar (◇). Data acquired with weaker focusing (35% larger f number) are shown in green (gray) and those obtained with tighter focusing (also in main figure) are in black.

species, the higher IP ions are produced in spatial regions with larger gradient fields (see Fig. 1). We propose that the observed reduction in normalized Rydberg yield for ions with higher IPs is due, almost entirely, to gradient-field ionization of Rydberg ions. Indeed, analogous measurements performed at similar intensities but with a more weakly focused beam show consistently larger normalized Rydberg yields (see inset of Fig. 3). The numerical simulation (solid curves in Fig. 3) described below supports our hypothesis and treats the creation of Rydberg ions and their exposure to the pondermotive gradient field as a sequential, two-step process.

To simulate the experiment, we first approximate the probability for creating bare and Rydberg ions as a function of intensity and then use the measured laser intensity distribution to determine the gradient field and ion densities throughout the focal volume. Next, we employ an impulsive, gradient-field ionization model to determine the n-dependent Rydberg ion survival probability at each point in the focus. Simulated ion yields are then computed by integrating the surviving Rydberg- and bare-ion densities over the laser focal volume.

Efficient excitation of Rydberg electrons requires a laser intensity greater than the saturation intensity for producing singly charged Xe, Kr, or Ar ions. These saturation intensities exceed 10^{14} W/cm^2, with associated pondermotive shifts greater than 6 eV. Given the magnitude of these energy shifts, the precise location of Rydberg resonances in the different species cannot be important in determining the efficiency of the Rydberg excitation. Therefore, we approximate the probability for producing a highly excited ion, $A^{(Z-1)+*}$, as

$$P_{(I,A^{(Z-1)+},n)} = CP_{(I,A^{Z+})}n^{-3}/\epsilon, \quad (1)$$

where C is a constant, $P_{(I,A^{Z+})}$ is the ADK tunneling probability for creating a bare ion A^{Z+}, and n^{-3}/ϵ is the probability that a Rydberg electron is produced in the energy interval n^{-3} between adjacent n states. $\epsilon = IP_{A^+} + 2U_{P_s}$ is the "Simpleman's" approximation for the range of electron energies (bound and continuum) resulting from the exposure of a neutral atom A to an intense laser pulse at the saturation intensity, I_s, for single ionization [14]. Equation (1) implicitly assumes that most Rydberg ions are created via inner electron ionization of neutral Rydberg atoms. The increased IP and saturation intensity for higher ionization stages ensures that $\epsilon_{Z>1} \gg \epsilon_{Z=1}$, so direct Rydberg ion excitation should be less probable for $Z > 1$. However, the explicit form of the normalization factor is not critical, and the simulation results are qualitatively similar if the normalization factor n^{-3}/ϵ is omitted.

The singly and doubly charged Rydberg ions that can be detected by field ionization in the TOF spectrometer have principle quantum numbers $28 < n < 90$ and $37 < n < 122$, respectively, and associated Kepler periods $\tau_K = 2\pi n^3/Z^2 > 800$ fs. Since $\tau_K \gg \tau_L$, once launched from the nucleus, Rydberg electrons travel far from the ion core and do not return until long after the laser pulse has passed. Consequently, the Rydberg *photoionization probability* is negligibly small, regardless of the local laser intensity and ion species [11]. The preceding arguments implicitly ignore the possibility that Rydberg electrons are driven back to the nucleus by the intense laser field. The fact that electrons with energies $<2U_P$ dominate the electron energy spectra from intense laser ionization of these atoms indicates that this electron rescattering probability is small [15].

The gradient field is derived from the laser intensity so, at any position within the laser focus, F_∇ takes the form of a brief, unipolar electric field pulse [16,17]. This "half-cycle" gradient-field pulse has a time-dependent field amplitude that is proportional to the temporal intensity profile of the laser pulse. Since $\tau_L \ll \tau_K$ for all detectable Rydberg ions, gradient-field ionization proceeds impulsively rather than adiabatically. The electron receives a momentum "kick" from F_∇, $\Delta p = F_0\tau_L$, where F_0 is the peak gradient field at the location of the Rydberg ion [18]. Quantum mechanically, the probability that the electron is ionized depends on its momentum distribution, its energy, and the kick strength Δp [18].

Neither the exact time at which the Rydberg wave packet is produced nor its precise momentum distribution are known. However, the n-dependent Rydberg survival probability can be approximated as follows. First, as discussed previously, it is likely that Rydberg ions are created through inner electron ionization of neutral Rydberg atoms. These excited atoms are produced early in the laser pulse, at intensities significantly lower than those required to saturate the ionization yields for the higher charge states. Therefore, we assume that all Rydberg states are populated on the leading edge of the laser pulse and experience a gradient field with FWHM duration, τ_L. This choice is not critical and qualitatively similar results are obtained if the impulse duration is chosen to be larger or smaller by factors of 2 or so. Second, an impulse $\Delta p_c = Z/n$ will impart an energy, $\Delta E = \Delta p_c^2/2 = Z^2/(2n^2) = E_0$ that is just sufficient to ionize a Rydberg electron with energy $-E_0$ and no momentum in the kick direction. An electron with the same initial energy, but moving with (against) the kick, will experience an energy gain $\Delta E > E_0$ ($\Delta E < E_0$) from the same impulse. Therefore, a Rydberg ion $A^{(Z-1)+*}$, with energy $-E_0$ and no preferred orientation for electronic orbital motion, will ionize with 50% probability when exposed to an impulse, Δp_c. Hence, we define the gradient-field ionization threshold for state n, $F_{0_c} = (\Delta p_c)/\tau_L = Z/(n\tau_L)$.

At low intensities, $I < 10^{15}$ W/cm^2, the gradient field has insufficient magnitude to strip the Rydberg ions, and the predicted normalized Rydberg yields are constant for each species (see Fig. 3). However, above some threshold intensity, gradient-field ionization results in a pronounced decrease in the normalized Rydberg yields. As expected, Rydberg ions with higher IPs are affected to a greater extent. With the exception of the Xe^{2+*}:Xe^{3+} ratio, the agreement between the data and simulation is good. The single, species-independent normalization constant, $C = 4.5$ in Eq. (1), has been adjusted to give the best agreement between all six simulation curves and the experimental data. The other inputs to the numerical code are obtained through direct measurement or are based on the physical arguments described above.

In summary, we have obtained what we believe is the first experimental evidence for the ionization of bound electrons in the gradient of the pondermotive potential in an intense focused laser beam. Rydberg ions, produced during intense laser ionization of noble gas atoms, are found to be excellent probes of the gradient-field ionization process. In general, our experimental data are in good agreement with the results of a numerical simulation that incorporates the gradient-field ionization mechanism. Importantly, the data and calculation disagree by up to 2 orders of magnitude if this effect is neglected. Independent evidence for the gradient-field ionization effect is obtained from our observation that the normalized Rydberg yields are greater in a more weakly focused beam geometry. Interestingly, we observe a normalized Xe^{2+*} Rydberg yield that is a factor of 2 larger than the normalized Xe^{2+*} signal and a factor of 4 larger than expected from the simulation. At the present, we are unaware of any single electron effect that could produce this anomaly and, therefore, we speculate that some multielectron mechanism is responsible.

This work is supported by the Chemical Sciences, Geosciences, and Biosciences Division, Office of Basic Energy Sciences, Office of Science, U.S. DOE, and the UVa FEST.

*Email address: rrj3c@virginia.edu

[1] P. M. Paul *et al.*, Science **292**, 1689 (2001); M. Hentschel *et al.*, Nature (London) **414**, 509 (2001).
[2] G. N. Gibson, Phys. Rev. Lett. **89**, 263001 (2002).
[3] T. Ditmire *et al.*, Nature (London) **398**, 489 (1999).
[4] J. Muth-Bohm *et al.*, Phys. Rev. Lett. **85**, 2280 (2000); C. Guo, *ibid.* **85**, 2276 (2000); M. J. DeWitt, E. Wells, and R. R. Jones, *ibid.* **87**, 153001 (2001).
[5] R. R. Jones, Phys. Rev. Lett. **74**, 1091 (1995); P. Hansch and L. D. Van Woerkom, Opt. Lett. **21**, 1286 (1996).
[6] See, for example, A. Ashkin *et al.*, Opt. Lett. **11**, 288 (1986);J. J. McClelland *et al.*, Science **262**, 877 (1993); H. Stapelfeldt *et al.*, Phys. Rev. Lett. **79**, 2787 (1997); K. M. O'Hara *et al.*, *ibid.* **82**, 4204 (1999).
[7] P. L. Kapitza and P. A. M. Dirac, Proc. Cambridge Philos. Soc. **29**, 297 (1933).
[8] P. H. Bucksbaum, D. W. Schumacher, and M. Bashkansky, Phys. Rev. Lett. **61**, 1182 (1988); D. L. Freimund, K. Aflatooni, and H. Batelaan, Nature (London) **413**, 142 (2001).
[9] The effect of the pondermotive gradient-force on free electrons is also seen in "long-pulse" above-threshold ionization (ATI) spectra. See T. J. McIlrath, *et al.*, Phys. Rev. A **35**, 4611 (1987).
[10] R. R. Freeman *et al.*, Phys. Rev. Lett. **59**, 1092 (1987).
[11] R. R. Jones, D. W. Schumacher, and P. H. Bucksbaum, Phys. Rev. A **47**, R49 (1993).
[12] R. B. Vrijen and L. D. Noordam, J. Opt. Soc. Am. B **13**, 189 (1996).
[13] E. Wells, M. J. DeWitt, and R. R. Jones, Phys. Rev. A **66**, 13409 (2002).
[14] N. B. Delone and V. P. Krainov, *Multiphoton Processes in Atoms* (Springer-Verlag, Berlin, 1999), 2nd ed., and references therein.
[15] G. G. Paulus *et al.* Phys. Rev. Lett. **72**, 2851 (1994).
[16] F_∇ also has a full-cycle component due to the forward propagation of the laser pulse through the laser focus. However, no net impulse is delivered to a free electron by this rapid transient, and, therefore, its effect is expected to be negligible.
[17] R. R. Jones, D. You, and P. H. Bucksbaum, Phys. Rev. Lett. **70**, 1236 (1993).
[18] R. R. Jones, Phys. Rev. Lett. **76**, 3927 (1996).